Influence of an inner core on the long-period forced librations of Mercury

Marie Yseboodt[a,*], Attilio Rivoldini[a], Tim Van Hoolst[a], Mathieu Dumberry[b]

[a]*Royal Observatory of Belgium, 3 Avenue Circulaire, 1180 Brussels, Belgium, +32 2 790 39 52*
[b]*Department of Physics, University of Alberta, Edmonton, T6G 2E1, Canada*

Abstract

The planetary perturbations on Mercury's orbit lead to long-period forced librations of Mercury's mantle. These librations have previously been studied for a planet with two layers: a mantle and a liquid core. Here, we calculate how the presence of a solid inner core in the liquid outer core influences the long-period forced librations. Mantle-inner core coupling affects the long-period libration dynamics mainly by changing the free libration: first, it lengthens the period of the free libration of the mantle, and second, it adds a second free libration, closely related to the free gravitational oscillation between the mantle and inner core. The two free librations have periods between 2.5 and 18 y depending on the internal structure. We show that large amplitude long-period librations of 10's of arcsec are generated when the period of a planetary forcing approaches one of the two free libration periods. These amplitudes are sufficiently large to be detectable by spacecraft measurements of the libration of Mercury. The amplitudes of the angular velocity of Mercury's mantle at planetary forcing periods are also amplified by the resonances, but remain much smaller than the current precision of Earth-based radar observations unless the period is very close to a free libration period. The inclusion of mantle-inner core coupling in the rotation model does not significantly improve the fit to the radar observations. This implies that it is not yet possible to determine the size of the inner core of Mercury on the basis of available observations of Mercury's rotation rate. Future observations of the long-period librations may be used to constrain the interior structure of Mercury, including the size of its inner core.

Keywords: Mercury, Planetary dynamics, Resonances, spin-orbit, Mercury, interior

Introduction

Mercury has a peculiar rotation: three rotation periods correspond to two revolution periods. This spin-orbit resonance leads to interesting physical phenomena such as the longitudinal librations. The librations are caused by the non-spherical mass distribution of Mercury, on which the Sun exerts a gravitational torque. The difference between the orbital and the rotation periods leads to a varying torque along the orbit since the orientation of the long axis of Mercury changes with respect to the direction to the Sun. Eccentricity further contributes to the variability by causing changes in the distance to the Sun and in the orbital speed. The main libration has a period of 87.97 days, equal to Mercury's orbital (annual) period, and an amplitude of 38.5 ± 1.6 arcsec (Margot et al., 2012). In addition, there are smaller amplitude librations at harmonic (semi-annual, ter-annual,...) frequencies. Those librations depend on the interior structure, notably the presence and the size of a liquid core inside the planet. By measuring the librations, we can infer knowledge about the interior structure. For example, by measuring Mercury's 88d libration amplitude, Margot et al. (2007) concluded that Mercury has a large liquid core. Since a magnetic field has been detected by the Mariner 10 spacecraft (e.g. Ness et al., 1975), it is thought that Mercury may have a solid inner core inside its liquid core. Peale et al. (2002) and Veasey and Dumberry (2011) have investigated the consequence of the addition of a solid inner core on the rotation dynamics of Mercury. Recently, Van Hoolst et al. (2012) showed that, if the inner core is larger than about 1000 km, the difference on the 88d libration amplitude may be non-negligible, and of the same order as the present uncertainty, about 1.5 as.

Another forced libration results from planetary perturbations. The periodic force arising from the gravitational interaction of a planetary body with Mercury causes a perturbation of Mercury's orbital motion, changing its position relative to the Sun and thus altering the solar torque acting on its equatorial bulge. This is an indirect effect of the planets on the rotation of Mercury. These long-period forced librations induced by the planetary perturbations have been predicted by e.g. Dufey et al. (2008), Peale et al. (2009) and Yseboodt et al. (2010). They have periods commensurate with the orbital revolution of the planets involved and are expected to have small amplitudes

---

*Corresponding author
Email address:* `m.yseboodt@oma.be` (Marie Yseboodt)

unless their period is close to the period of a free libration in which case a near-resonant amplification can occur. In the absence of an inner core, there is only one such mode, the free mantle libration. This mode describes an oscillation of the axis of minimum moment of inertia about the Mercury-Sun line at perihelion (Peale, 2005). The period of the free mantle libration depends on the moments of inertia of Mercury, and is approximately 12 years. This is very close to Jupiter's perturbation on Mercury's orbit at 11.86y; Dufey et al. (2008) and Peale et al. (2009) have shown that a forced libration of 20 arcsec or more can be generated, the exact amplitude depending on the moments of inertia. Besides this 11.86y forced libration, at least 4 other long-period forced librations have amplitudes larger than the arcsecond level.

The previous studies on the long-period forced librations assumed no mantle-inner core coupling. Adding an inner core has two effects on the free libration: First, as shown by Peale et al. (2002), Veasey and Dumberry (2011) and Van Hoolst et al. (2012), it can lengthen the period of the free libration of the mantle since the motion of the mantle is locked to that of the inner core for this mode. As a result, interior models with a large inner core may no longer have a free period close to Jupiter's orbital period. Second, the presence of the inner core adds a second free libration, closely approximated by the free gravitational oscillation between the mantle and inner core, and thus the possibility of additional resonances at other orbit perturbation frequencies.

In this study, we investigate how a non-spherical inner core coupled to the mantle and the outer core may influence the long-period forced librations. Since planetary perturbation periods may be close to the period of the two free modes, the long-period librations may be resonantly enhanced and this may lead to a rotation angle that substantially differs from a model where there is no solid inner core. The presence of the solid inner core affects the rotation state of Mercury and may result in a signature that is detectable in the observations, in which case it must be taken into account when analyzing the data. In our rotation model, we also take into account the dissipation since this effect reduces the libration amplitudes and introduces phase lags. We include viscous and electromagnetic coupling at the core-mantle and inner-outer core boundaries, as well as the effect of viscous deformation within the inner core. The signature of the parameters responsible for the dissipation on the libration is discussed.

In the theory section, we derive equations for the amplitude of the long-period forced librations of the mantle and of the inner core. The equations are given for cases with and without dissipation. We then numerically evaluate these libration equations on the basis of recent interior models of Mercury's (Rivoldini et al., 2009) (section 1.7). The results are compared for different interior models. In the results section (section 2), we show that the amplitude of the long-period librations are of the order of a few arcsec, and much larger if the forcing period approaches the period of one of the free modes. In the last section (section 3), we compare predictions of libration models with and without mantle-inner core coupling with the Earth-based radar observations of the rotation rate of Mercury of Margot et al. (2012) in order to determine whether the size of the inner core can be determined on the basis of the currently available radar data.

1. Theory

1.1. Equations of motion for the mantle and the solid inner core

We assume an equatorial flattened bi-axial model of Mercury with a silicate shell composed of the mantle and the crust (we use the symbol m for the shell), a fluid outer core (oc) and the solid inner part of the core (ic). If the mantle and the inner core have a different rotation, their principal axes of inertia will be misaligned and there will be an effect of the gravitational and pressure coupling between these layers (see for example Van Hoolst et al. 2012). The librational motion of the mantle and the solid inner core can be described by considering the change in angular momentum of these layers as a result of the external torque of the Sun and the internal torques. For the libration equation, we assume that the mantle and inner core are rigid solids as the effect of elastic deformations has been shown to be below the observational detection limit (Van Hoolst et al., 2012). We then have the equations of motion:

$$\ddot{\psi}_m = -\frac{GM_S}{C_m \, r^3 \, n^2} \, K_m \, \sin 2\left(\psi_m - \varpi - f\right) - \frac{K}{C_m} \sin 2\left(\psi_m - \psi_{ic}\right) , \tag{1}$$

$$\ddot{\psi}_{ic} = -\frac{GM_S}{C_{ic} \, r^3 \, n^2} \, K_{ic} \, \sin 2\left(\psi_{ic} - \varpi - f\right) + \frac{K}{C_{ic}} \sin 2\left(\psi_m - \psi_{ic}\right) . \tag{2}$$

The rotation angle of the mantle ψ_m describes the orientation of the axis of minimum moment of inertia of the mantle A_m relative to the intersection between the ecliptic and the orbital plane at J2000. Similarly, ψ_{ic} is the rotation angle of the inner core. f is the true anomaly, ϖ the longitude of the pericenter, r the distance between the mass centers of Mercury and the Sun, $A_{ic} < B_{ic} < C_{ic}$ are the principal moments of inertia of the inner core and $A_m < B_m < C_m$ the mantle moments of inertia. n is the mean motion of Mercury, M_S the mass of the Sun and G the gravitational constant. The factors K_m and K_{ic} describe the strengths of the gravitational and pressure torques on the mantle and inner core, respectively (Van Hoolst et al., 2012; Dumberry et al., 2013). These factors are defined by $K_m = \frac{3}{2} n^2 \left(B_m - A_m + B_{oc,t} - A_{oc,t}\right)$ and $K_{ic} = \frac{3}{2} n^2 \left(B_{ic} - A_{ic} + B_{oc,b} - A_{oc,b}\right)$, where $A_{oc,b}$ and $B_{oc,b}$ are the principal moments of inertia of the bottom part of the fluid core (a layer between the inner core-outer core boundary (ICB) and the smallest sphere that can be included in the fluid core, see Fig. 2 of Van Hoolst

et al. 2008) while $A_{oc,t}$ and $B_{oc,t}$ are related to the rest of the fluid core. The terms proportional to $B_m - A_m$ and $B_{ic} - A_{ic}$ capture the solar gravitational torques on the mantle and inner core, respectively. The additional terms arise from the pressure torques on the boundaries between the outer core and mantle and between the inner core and outer core. It can be shown that in the limit of no inner core, the expression of K_m reduces to $(3/2)\,n^2(B - A)$, and we retrieve the classical equation of a planet with two layers. K is the gravitational-pressure coupling constant between the mantle and the inner core. If the inner and outer parts of the core have uniform density ρ_j ($j = oc$ for the fluid outer core, $j = ic$ for the solid inner core and $j = m$ for the silicate shell), K is defined by (e.g. Veasey and Dumberry, 2011)

$$K = \frac{4\pi G}{5}\left(1 - \frac{\rho_{oc}}{\rho_{ic}}\right) C_{ic}\,\beta_{icb}\left[(\rho_{oc} - \rho_m)\,\beta_{cmb} + \rho_m \beta_m\right],$$
(3)

where β_m, β_{cmb} and β_{icb} are the geometrical equatorial flattenings at the top of the mantle, core-mantle boundary (CMB) and ICB, respectively. If an ellipsoidal surface of constant density at a given radius has its three principal semi-axes defined by $a > b > c$, the geometrical flattening in the equatorial plane is defined by $\beta = (a - b)/a$. For the computation of the longitudinal librations, the polar flattening may be neglected. When radial density variations in both the fluid and solid cores are taken into account, the expression for K is more complicated and given in Dumberry et al. (2013). Since the effect of the small obliquity on the longitudinal librations is below the observational detection limit, the obliquity of Mercury is assumed to be 0 (its true value is 0.034°, Margot et al. 2012) so that Mercury's equator and orbit are the same plane.

Previous studies of the effect of the inner core on Mercury's rotation focused on the amplitude of the 88d librations and considered a Kepler orbit, in which the orbital elements are constant with time, except for the true and the mean anomalies. In order to derive differential equations that use a small angle, the rotation angle ψ_m is usually related to the mantle libration angle γ_m with the relation $\psi_m = \gamma_m + 1.5\,M$, where $M = n(t - t_0)$ is the mean anomaly of the orbital motion and t_0 is a chosen initial time. A similar expression is used to relate ψ_{ic} and γ_{ic}, the libration angles of the inner core.

When long-period librations are considered, the longitude of the pericenter ϖ is no longer constant with time while the true anomaly $f(t)$ and the distance between Mercury and the Sun $r(t)$ have a quasiperiodic evolution because of the planetary perturbations that affect the orbit of Mercury. Following Yseboodt et al. (2010) we define the mantle libration angle γ_m and an inner core libration angle γ_{ic} by

$$\psi_m = \gamma_m + 1.5\,M + \varpi = \gamma_m + \lambda,$$
(4)
$$\psi_{ic} = \gamma_{ic} + 1.5\,M + \varpi = \gamma_{ic} + \lambda,$$
(5)

where the angle λ is defined by $1.5\,M + \varpi$. All these an-

gles are functions of time. The angle λ can be written as a sum of the mean rotation and a frequency decomposition $\lambda(t) = 1.5\,n\,t + 1.5\,M(t_0) + \varpi(t_0) + \dot{\varpi} + \sum_i \lambda_i \cos(\omega_i t + \phi_{\lambda_i})$ where λ_i, ω_i and ϕ_{λ_i} are the amplitude, angular frequency and phase of the different planetary perturbations on Mercury's orbit. The origin of the angles ψ_m and ψ_{ic} is defined by a fixed line with respect to an inertial frame, while the origin of the γ_m and γ_{ic} angles is moving because of the planetary perturbations (see figure 1 in Yseboodt et al. 2010). Only ψ_m can be observed although the libration angle of the mantle γ_m is more convenient mathematically because it is a small quantity.

To compute the long-period forced librations, the differential equations (1) and (2) are expanded as two functions of the mean anomaly and of the eccentricity. Since we study the long-period librations, we discard the terms containing the mean anomaly of Mercury in the right hand side of the equations. However terms containing the second time derivative of the mean anomaly and the longitude of the pericenter ($\ddot{\varpi}(t)$) remain in the left hand side of the equations (Yseboodt et al., 2010). The angles γ_m and γ_{ic} are usually small, so that the small angle approximation can also be used. We get two linearized equations for γ_m and γ_{ic} that contain the planetary perturbations on the orbit of Mercury

$$\ddot{\gamma}_m - \sum_i \omega_i^2 \lambda_i \cos(\omega_i t + \phi_{\lambda_i}) = -\omega_m^2\,\gamma_m - \frac{2K}{C_m}\left(\gamma_m - \gamma_{ic}\right),$$
(6)
$$\ddot{\gamma}_{ic} - \sum_i \omega_i^2 \lambda_i \cos(\omega_i t + \phi_{\lambda_i}) = -\omega_{ic}^2\,\gamma_{ic} + \frac{2K}{C_{ic}}\left(\gamma_m - \gamma_{ic}\right),$$
(7)

where the frequencies ω_m and ω_{ic} are given by

$$\omega_m^2 = 2\,f_2\,\frac{K_m}{C_m},$$
(8)
$$\omega_{ic}^2 = 2\,f_2\,\frac{K_{ic}}{C_{ic}},$$
(9)

and where f_2 is a function of the eccentricity ($f_2(e) = \frac{7}{2}e - \frac{123}{16}e^3 + \cdots$).

In the linearized equations (6) and (7), the planetary perturbations are not included as a torque acting on the mantle and the inner core (this direct effect is negligible because of the large distance between Mercury and the other planets) but appear as an indirect effect, through the definition of the γ angles. This additional term, coming from the time derivative of the angle ψ_m, acts like a "forcing" in the differential equations. In the limit of no inner core, $K = 0$ and Eq. (8) becomes the usual expression of the free mantle libration frequency

$$\omega_{m\text{ no ic}}^2 = 3\,n^2\,f_2\,(B - A)/C_m.$$
(10)

1.2. Planetary perturbations from the ephemerides

Using the JPL DE405/DE406 ephemerides (Standish, 1998) over a period of about 1000 years before and after J2000 and performing a frequency analysis, we get

3

the frequencies ω_i, amplitudes λ_i and phases ϕ_{λ_i} of the main planetary perturbations on Mercury's orbit (see Table 1). We use the frequency mapping FAMOUS software (ftp://ftp.obs-nice.fr/pub/mignard/Famous).

Period $2\pi/w_i$ (y)	Forcing argument	λ_i (as)	ϕ_{λ_i} (deg)	$\psi_{m\,i}$ (as)
3.955	Jupiter $(3\lambda_J)$	0.45	35	0.1
5.663	Venus $(2\lambda_M - 5\lambda_V)$	12.7	87	3.9
5.932	Jupiter $(2\lambda_J)$	4.31	4	1.5
6.574	Earth $(\lambda_M - 4\lambda_E)$	1.37	332	0.6
11.861	Jupiter (λ_J)	1.40	171	38.4
14.727	Saturn $(2\lambda_S)$	0.52	36	1.4
1.110	$(\lambda_M - 2\lambda_V)$	7.59	235	0.1
0.555	$(2\,\lambda_M - 4\lambda_V)$	1.01	17	0.0
0.292	$(2\,\lambda_M - 3\lambda_V)$	0.99	305	0.0
0.465	$(\lambda_M - 2\lambda_E)$	0.88	38	0.0
0.251		0.79	172	0.0
0.396	$(\lambda_M - \lambda_V)$	0.72	160	0.0
0.615	(λ_V)	0.65	16	0.0
0.198		0.64	231	0.0
0.241		0.62	86	0.0
1.380	$(\lambda_M - 3\lambda_V)$	0.40	222	0.0

Table 1: Planetary perturbations of Mercury's orbit and frequency decomposition of the $\lambda = 1.5\,M + \varpi$ angle. The last column shows the amplitude of the librations (rotation angle ψ_m, see Eq. (15)) if $(B-A)/C_m = 2.18 \times 10^{-4}$ (Margot et al., 2012) and if there is no mantle-inner core coupling. The six perturbation frequencies that may be resonantly amplified by free librations are listed above the horizontal line.

Table 1 is an updated version of Table 1 in Yseboodt et al. (2010). Some typos have been corrected and some values are slightly altered because we use a different time interval for the ephemerides. Using another ephemerides will also slightly change these values. In the second column we give the source of the planetary perturbation (forcing argument). Note that the origin of some of these perturbations (mostly the periods smaller than 100 days) cannot be identified unambiguously and are left blank; these do not match exactly a known orbital frequency and may represent the combined effect from many closely separated frequencies. The main planetary perturbations have periods that range from approximately twenty days to fifteen years and the amplitudes of the λ angle are as high as 12.7 as.

1.3. The eigenmodes

The frequencies of the eigenmodes are found by solving for the roots of the characteristic equation $\omega^4 - 2\,\omega^2\,\omega_a^2 + \left(\omega_{ic}^2\,\alpha_m^2 + \omega_m^2\,\alpha_{ic}^2 + \omega_m^2\,\omega_{ic}^2\right) = 0$ of Eqs. (6) and (7) (Dumberry, 2011; Van Hoolst et al., 2012)

$$\omega_{1,2}^2 = \omega_a^2 \mp \sqrt{\omega_a^4 - (\omega_{ic}^2\,\omega_m^2 + \omega_m^2\,\alpha_{ic}^2 + \omega_{ic}^2\,\alpha_m^2)}, \quad (11)$$

where

$$\omega_a^2 = \frac{\omega_g^2 + \omega_m^2 + \omega_{ic}^2}{2}, \quad \omega_g^2 = \frac{2K(C_m + C_{ic})}{C_{ic}\,C_m}, \quad (12)$$

$$\alpha_m^2 = \frac{2K}{C_m}, \quad \alpha_{ic}^2 = \frac{2K}{C_{ic}}. \quad (13)$$

Note that the frequencies of the free modes are independent of the planetary perturbations.

Free modes are natural solutions of the libration equations and, if excited by some process, may have arbitrary large amplitudes. Dissipation is undoubtedly present (and will be discussed in section 1.5) and will attenuate the amplitude of the free librations in time on a timescale much smaller than the age of the Solar System (Peale, 2005). So if free modes are part of Mercury's librations, they require a recent or on-going excitation. The most recent analysis of Mercury's spin rate observations suggests that a libration model that includes a free mantle libration does not significantly improve the fit to observations (Margot et al., 2012). However, the spin rate variations associated with a decadal free librations of a few 10's of arcsec are much smaller than those caused by the much more rapid 88d libration. Thus, it is difficult to rule out conclusively the presence of free librations on the basis of spin rate data alone. Robust conclusions on the amplitude (and period) of the free librations must await future observations, especially observations of the long term changes in the angle of libration.

1.4. The amplitude of the undamped long-period forced librations

Without mantle-inner core coupling and without dissipation but taking into account the planetary perturbations on the orbit of Mercury, the analytical solution of the linearized differential equation (6) for the long-period forced libration of the mantle is (Yseboodt et al., 2010)

$$\gamma_m(t) = \sum_i \lambda_i \frac{\omega_i^2}{\omega_m^2 - \omega_i^2} \cos(\omega_i t + \phi_{\lambda_i}), \quad (14)$$

or the long-period forced librations for the rotation angle ψ_m

$$\psi_m(t) = \sum_i \lambda_i \frac{\omega_m^2}{\omega_m^2 - \omega_i^2} \cos(\omega_i t + \phi_{\lambda_i}) \cdot \quad (15)$$

The long-period forced librations have angular frequencies ω_i equivalent to the orbital frequencies.

The expression for the forced librations of the inner core $\gamma_{ic}(t)$ including planetary perturbations but neglecting any coupling between the mantle and the inner core is very similar to the expression $\gamma_m(t)$, the ω_m frequency being replaced by ω_{ic}. The inner core free libration (see Eq. (9)) has a period of about $50 - 60$y.

If the effect of mantle-inner core coupling on the libration and the planetary perturbations on the orbit are

4

included, the forced part of the solution for γ_m and γ_{ic} of Eqs. (6) and (7) are

$$\gamma_m(t) = \sum_i \lambda_i \frac{\omega_g^2 + \omega_{ic}^2 - \omega_i^2}{(\omega_1^2 - \omega_i^2)(\omega_2^2 - \omega_i^2)} \omega_i^2 \cos(\omega_i t + \phi_{\lambda_i}),$$

(16)

$$\gamma_{ic}(t) = \sum_i \lambda_i \frac{\omega_g^2 + \omega_m^2 - \omega_i^2}{(\omega_1^2 - \omega_i^2)(\omega_2^2 - \omega_i^2)} \omega_i^2 \cos(\omega_i t + \phi_{\lambda_i}) \cdot$$

(17)

By using Eq. 4, the rotation angle ψ_m of the mantle can be written as

$$\psi_m(t) = \sum_i \lambda_i \frac{\alpha_m^2 \omega_{ic}^2 + \omega_m^2(\alpha_{ic}^2 + \omega_{ic}^2 - \omega_i^2)}{(\omega_1^2 - \omega_i^2)(\omega_2^2 - \omega_i^2)} \cos(\omega_i t + \phi_{\lambda_i}),$$

(18)

$$= \sum_i \lambda_i \left(\frac{N}{\omega_1^2 - \omega_i^2} + \frac{\omega_m^2 - N}{\omega_2^2 - \omega_i^2} \right) \cos(\omega_i t + \phi_{\lambda_i}),$$

(19)

where

$$N = \frac{\omega_m^2}{2} + \frac{\omega_m^2(\alpha_{ic}^2 - \alpha_m^2 - \omega_m^2 + \omega_{ic}^2) + 2\alpha_m^2 \omega_{ic}^2}{4\sqrt{\omega_a^4 - (\omega_{ic}^2 \omega_m^2 + \omega_m^2 \alpha_{ic}^2 + \omega_{ic}^2 \alpha_m^2)}} \cdot$$

(20)

By comparing Eqs. (15) and (18), we notice the second eigenfrequency in the denominator and a different numerator of the libration amplitude, while the dependence on the planetary perturbation λ_i and the temporal behavior with the frequency and the phase do not change. In Eq. (19), the two terms inside the parenthesis represent the resonance factors associated with each of the two free librations. In this expression of the libration amplitude for the rotation angle ψ_m, the forcing frequency dependence is in the denominators only. Additionally, for an equivalent offset to the resonance frequency, a larger numerator of the resonance factor indicates a stronger resonance effect. The resonance with the first eigenfrequency usually has a larger effect than the second eigenfrequency.

1.5. The damped long-period forced librations

Dissipation at the CMB from viscous or electromagnetic (EM) coupling between the mantle and the fluid core is proportional to their differential rotation rate. The effect of dissipation on libration is included by adding a term $-k_m(\dot{\gamma}_m - \dot{\gamma}_{oc})$ on the right-hand side of Eq. (6), where k_m is a damping coefficient (e.g. Peale, 2005) and γ_{oc} is the libration angle of the fluid core (and $\dot{\gamma}_{oc}$ its time-derivative). Likewise, dissipation at the ICB is introduced by including a term $-k_{ic}(\dot{\gamma}_{ic} - \dot{\gamma}_{oc})$ on the right-hand side of Eq. (7), where k_{ic} is a damping coefficient at the ICB. Because of the dissipative interaction of the outer core with the mantle and the inner core, the outer core will also librate and a third equation, the evolution of the libration of the fluid core, is required to solve the system. We also add the dissipation from viscous deformation within the inner core. We

follow Koning and Dumberry (2013) and assume an inner core with a simple Newtonian rheology with viscous deformation taking place over a characteristic e-folding time of τ. This adds a term $-\tau^{-1}(\dot{\gamma}_{ic} - \dot{\gamma}_m)$ on the right-hand side of Eq. (7).

It is more convenient to re-write the forcing term in Eqs. (6-7) as

$$\omega_i^2 \lambda_i \cos(\omega_i t + \phi_{\lambda_i}) = \omega_i^2 \left(f_i e^{-I\omega_i t} + f_i^* e^{I\omega_i t} \right),$$

(21)

where f_i^* is the complex conjugate of f_i and $I = \sqrt{-1}$. The real and imaginary parts of f_i are related to λ_i and ϕ_{λ_i} by

$$\mathrm{Re}[f_i] = \frac{1}{2}\lambda_i \cos\phi_{\lambda_i},$$

(22)

$$\mathrm{Im}[f_i] = -\frac{1}{2}\lambda_i \sin\phi_{\lambda_i}.$$

(23)

Since equations (6-7) are linear in the libration angles γ_m and γ_{ic}, we can find the solutions to the forcing f_i (at frequency ω_i) and that to the forcing f_i^* (at frequency -ω_i) individually and add up their solution. Let us do the f_i part. The equations of motion for the mantle, fluid outer core and solid inner core are now

$$\ddot{\gamma}_m + \omega_m^2 \gamma_m + \alpha_m^2(\gamma_m - \gamma_{ic}) + k_m(\dot{\gamma}_m - \dot{\gamma}_{oc}) = \omega_i^2 f_i,$$

(24)

$$\ddot{\gamma}_{oc} - \frac{C_m}{C_{oc}} k_m(\dot{\gamma}_m - \dot{\gamma}_{oc}) - \frac{C_{ic}}{C_{oc}} k_{ic}(\dot{\gamma}_{ic} - \dot{\gamma}_{oc}) = 0,$$

(25)

$$\ddot{\gamma}_{ic} + \omega_{ic}^2 \gamma_{ic} - \alpha_{ic}^2(\gamma_m - \gamma_{ic}) + k_{ic}(\dot{\gamma}_{ic} - \dot{\gamma}_{oc}) + \frac{\dot{\gamma}_{ic} - \dot{\gamma}_m}{\tau} = \omega_i^2 f_i.$$

(26)

Assuming periodic solutions of the form

$$\gamma_m(t) = \tilde{\gamma}_m e^{-I\omega_i t},$$

(27)

$$\gamma_{oc}(t) = \tilde{\gamma}_{oc} e^{-I\omega_i t},$$

(28)

$$\gamma_{ic}(t) = \tilde{\gamma}_{ic} e^{-I\omega_i t},$$

(29)

where $\tilde{\gamma}_m$, $\tilde{\gamma}_{oc}$, and $\tilde{\gamma}_{ic}$ are complex amplitudes, the system of equations (24-26) can be written as

$$\mathsf{A} \cdot \mathbf{x} = \mathbf{f},$$

(30)

where the matrix A contains the model parameters and vectors $\mathbf{x}$ and $\mathbf{f}$ contain the forced libration amplitudes and forcing, respectively,

$$\mathbf{x} = \begin{bmatrix} \tilde{\gamma}_m \\ \tilde{\gamma}_{oc} \\ \tilde{\gamma}_{ic} \end{bmatrix}, \qquad \mathbf{f} = \begin{bmatrix} \omega_i^2 f_i \\ 0 \\ \omega_i^2 f_i \end{bmatrix}.$$

(31)

The amplitude of libration ($\mathbf{x}$) at a given forcing frequency can be found by solving Eq. (30). The amplitude and phase of each of the mantle, inner core and fluid core libration can then be retrieved from the real and imaginary parts of the solution vector $\mathbf{x}$. For instance, the amplitude

of the mantle libration is $\sqrt{\operatorname{Re}[\tilde{\gamma}_m]^2 + \operatorname{Im}[\tilde{\gamma}_m]^2}$. To this, we must add the solution from the f_i^* part of the forcing: the solution is $\mathbf{x}^*$. So the total mantle amplitude is $2\sqrt{\operatorname{Re}[\tilde{\gamma}_m]^2 + \operatorname{Im}[\tilde{\gamma}_m]^2}$. If the phase of $\gamma_m(t)$ is defined as $\phi_{\lambda_i} + \phi_i^R$ (R like resonant), then the absolute value of the amplitude of the rotation angle ψ at frequency ω_i is

$$\tilde{\psi}_m = \sqrt{\tilde{\gamma}_m^2 + \lambda_i^2 + 2\tilde{\gamma}_m \lambda_i \cos \phi_i^R} \,, \qquad (32)$$

while the phase of the rotation angle ψ_m is given by

$$\tan \phi_{\psi_i} = \frac{\tilde{\gamma}_m \sin(\phi_{\lambda_i} + \phi_i^R) + \lambda_i \sin \phi_{\lambda_i}}{\tilde{\gamma}_m \cos(\phi_{\lambda_i} + \phi_i^R) + \lambda_i \cos \phi_{\lambda_i}} \,. \qquad (33)$$

The analytical expressions of $\tilde{\gamma}_m$, $\tilde{\psi}_m$ and its phase as a function of the different frequencies α_m, α_{ic}, ω_m and ω_{ic} can be derived, they are too long to be printed here.

The inclusion of dissipation alters the amplitude of the long-period forced librations given in Eqs. (16-18) and adds a phase lag between the planetary forcing and the response of the mantle, fluid core and inner core. The eigenfrequencies ω_1 and ω_2 are now complex. For small damping parameters (k_m and k_{ic} smaller than 10^{-3}/y, $\tau > 100$ years), the change in the real part of the eigenfrequencies is negligible. The introduction of dissipation through k_m and k_{ic} results in a finite amplitude of libration when the forcing period is equal to one of the free libration periods. The maximal amplitude of $\tilde{\psi}_m$ at the resonant frequency $\omega_i \approx \omega_1$ or ω_2 in the limit of a rigid inner core is approximately equal to

$$\tilde{\psi}_{m\,\text{MAX}} \approx \frac{\lambda_i}{\omega_i} \frac{\alpha_m^2 \omega_{ic}^2 + \alpha_{ic}^2 \omega_m^2 - \omega_m^2 \omega_i^2 + \omega_m^2 \omega_{ic}^2}{k_m \left(\alpha_{ic}^2 - \omega_i^2 + \omega_{ic}^2\right) + k_{ic}\left(\alpha_m^2 - \omega_i^2 + \omega_m^2\right)} \,. \qquad (34)$$

The amplitudes of the damping parameters k_m and k_{ic} depend on the nature of the coupling. For viscous coupling, using a molecular value of the kinematic viscosity of Mercury's fluid core of the order of 10^{-6} m^2/s (e.g., de Wijs et al., 1998), k_m and k_{ic} are both of the order of 10^{-5}/y (Peale, 2005). This validates the small damping approximation that led to expression (34).

Electromagnetic coupling at the CMB depends on the electrical conductivity of the lower mantle. If a conducting layer of thickness Δ and conductivity σ_m is present at the base of Mercury's mantle, then k_m^{EM} would be given by (e.g., Buffett, 1998)

$$k_m^{\text{EM}} = \frac{\sigma_m \Delta}{C_m} r_{cmb}^4 \mathcal{I}(B_r)_{\text{CMB}} \,, \qquad (35)$$

where $\mathcal{I}(B_r)_{\text{CMB}}$ is a factor that depends on the geometry of the radial magnetic field at the CMB and r_{cmb} is the CMB radius. For a simple dipole magnetic field of RMS amplitude B_r^d, $\mathcal{I}(B_r) = 64\pi (B_r^d)^2 / 15$ (Koning and Dumberry, 2013). Using a dipole field amplitude of 200 nT, of the same order as that observed by MESSENGER (Anderson et al., 2011) and a mantle conductivity $\sigma_m = 0.1$ S/m (e.g. Constable, 2007; Verhoeven et al., 2009), then even

if Δ is equal to the whole mantle thickness, k_m^{EM} is several orders of magnitude smaller than the viscous estimate above. If a layer of highly conducting material is present at the base of the mantle, as is inferred for Earth from nutation observations (e.g., Buffett, 1992) or at the top of the core of Mercury as it has been proposed by Smith et al. (2012), then k_m^{EM} can be larger. However, even if we use the terrestrial values of $\Delta = 200$ m and $\sigma_m = 10^6$ S/m, because the magnetic field of Mercury is weak, electromagnetic coupling remains weaker than viscous coupling. Electromagnetic coupling at the CMB can be neglected.

Electromagnetic coupling can be larger at the ICB because both the inner core and fluid core are good conductors. If we assume the same electrical conductivity σ on both the solid and fluid sides of the ICB, the EM coupling constant k_{ic}^{EM} can be written as (e.g., Buffett, 1998)

$$k_{ic}^{\text{EM}} = \frac{(1 + I)}{4\sqrt{\omega_i}} \frac{1}{C_{ic}} \sqrt{\frac{2\sigma}{\mu}} r_{icb}^4 \mathcal{I}(B_r)_{\text{ICB}} \,, \qquad (36)$$

where μ is magnetic permeability. The EM coupling parameter k_{ic}^{EM} is complex and frequency dependent. If we use a nominal ICB magnetic field of the same order as that at the CMB, and a 5y periodic forcing, then k_{ic}^{EM} is approximately 10^{-5}/y for $\sigma = 10^6$ S/m (Deng et al., 2013), of the same order as for viscous coupling. It is likely that the field at the ICB is larger than at the CMB, and if we use a factor 10 increase, then $k_{ic}^{\text{EM}} \approx 10^{-3}$/y. Although EM coupling would dominate viscous coupling in this "strong field" regime, the amplitude of k_{ic}^{EM} remains sufficiently small as to not lead to large variations in the period of the free librations calculated in the absence of dissipation (e.g. Dumberry, 2011). In all the calculations that we report in the results section, we use $k_m = k_{ic} = 10^{-5}$/y, unless otherwise noted.

Viscous dissipation within the inner core is difficult to evaluate because we do not know the viscosity of the inner core and hence, the characteristic timescale τ. However, if τ is shorter than 10^5y, then dissipation of the libration energy through viscous inner core deformation should dominate that from coupling at the CMB and ICB. Given that the temperature inside the inner core is likely not too far from the melting point, it is conceivable that τ may be as short as 10y. In the results section, we will report on the effect of using different values of τ in our calculations.

1.6. Harmonics of the 88d libration

In order to compare the model to the data, we need a rotation model that includes both the short-period and long-period forced librations. We use all harmonics of the 88d forced librations up to the 6th harmonic.

$$\gamma_m = \sum_i^7 g_i \sin(i\, n\, (t - t_{\text{pericenter}})) \cdot \qquad (37)$$

The amplitude g_i of the forced librations at the frequency $i\,n$ can be expressed as

$$g_i = (G_{2\,0\,1-i} - G_{2\,0\,1+i}) \cdot$$
$$\frac{i^2 n^2 C_m C_{ic}\, \omega_m^2 - C_m C_{ic}\, \omega_m^2 \omega_{ic}^2 - 2K C_m\, \omega_m^2 - 2K C_{ic}\, \omega_{ic}^2}{2 f_2\, C_m C_{ic}\, (i^2 n^2 - \omega_1^2)\,(i^2 n^2 - \omega_2^2)},$$
$$(38)$$

where the G_{jkl} are the eccentricity functions of Kaula (see Table 2 or Kaula (1966) for example).

i	$G_{2\,0\,1-i} - G_{2\,0\,1+i}$
1	$1 - 11e^2 + \frac{959\,e^4}{48} - \frac{3641\,e^6}{288}$
2	$-\frac{e}{2} - \frac{421\,e^3}{24} + \frac{32515\,e^5}{768}$
3	$-\frac{533\,e^4}{16} + \frac{13827\,e^6}{160}$
4	$\frac{e^3}{48} - \frac{57073\,e^5}{960}$
5	$\frac{e^4}{24} - \frac{18337\,e^6}{180}$
6	$\frac{81\,e^5}{1280}$
7	$\frac{4\,e^6}{45}$

Table 2: Eccentricity functions of the annual period and its first six harmonics, up to degree 6 in eccentricity.

Earth-based radar observations of Mercury yield estimates of the rotation rate variations. Because of the time derivative of the rotation rate that emphasizes the weight of the short period terms with respect to the rotation angle, the number of harmonics needed to precisely describe the temporal behavior of the rotation rate is larger than the numbers of harmonics of the libration angle model. The annual and the semi-annual amplitudes have been given in Van Hoolst et al. (2012). The ter-annual and the other small period libration amplitudes have been derived here using the same method. However, the effect of the inner core on the ter-annual and the other very short period is very small (smaller than 0.1 as for the libration angle or smaller than 1 as/y for the rotation rate).

If the effect of the coupling of the inner core and the mantle is neglected then Eq. (38) is reduced to the expression

$$g_i = \frac{(G_{2\,0\,1-i} - G_{2\,0\,1+i})}{i^2}\, \frac{3\,(B - A)}{2\,C_m - 6 f_2 (B - A)}. \qquad (39)$$

1.7. Interior model for Mercury and flattening of the layers

The amplitude of the long-period forced librations depends on the frequencies of the free modes $\omega_{1,2}$ as well as on ω_g, ω_m, ω_{ic}, α_m and α_{ic}. In turn, these quantities depend on the parameters K, K_m and K_{ic}, themselves being function of the moments of inertia of the mantle, fluid outer core and solid inner core. To determine these quantities, we first construct hydrostatic spherical interior models for Mercury with the method presented in Rivoldini et al. (2009) and an updated model for the core (Rivoldini et al., 2011; Rivoldini and Van Hoolst, 2013). The models have depth varying density profiles, resulting from compression and temperature variations. They are constrained to have the same mass, radius and mean moment of inertia as Mercury. The core of the models is made of iron and the light element sulfur and we use equations of state to compute the density as a function of depth. For each given core radius, the radius of the inner core is determined from the sulfur concentration, temperature and pressure inside the core, and from the iron-sulfur melting temperature. In this study we only consider models which have an inner core, however we note that models without an inner core are also compatible with observations. Likewise the core, for the mantle we solve equations of state to calculate the density as a function of depth. However, since the pressure increase with depth inside the mantle is small and since phase transitions to denser mineral phases are unlikely, we here neglect the small increase in density with depth and use a uniform density for the mantle (the average value of the depth dependent mantle density profile). Therefore, and as a consequence of mass conservation the average mantle density for models of the same mantle composition vary with mantle temperature, core radius, and inner core radius (see Table 3). Unlike for the mantle, compressibility effects in the core are significant and cannot be neglected. For the interior models we use 5 plausible mantle mineralogies that have been deduced from considerations about Mercury's formation and from the chemical composition of its surface (Verhoeven et al., 2009; Rivoldini et al., 2009). The temperature inside the core is assumed adiabatic and for the mantle we use a cold (T_{cmb}=1850K) and a hot temperature (T_{cmb}=2000K) profile that have been obtained from independent studies about the thermal evolution of Mercury (see the references in Rivoldini et al. 2009). These two values are representative of the lower and upper temperature range for Mercury from thermal evolution. Many other mantle mineralogies and temperature profiles are possible, in particular profiles with significantly lower temperatures (Grott et al., 2011). Therefore it has to be kept in mind that the interior models that we use only represent a subset of possible interior models. Among the different combinations of mineralogies and temperature profiles, 9 different classes of interior models fulfill the constraints on mass, radius and mean moment of inertia for some inner core radii (see Table 3). Interior models with a cold temperature profile fulfill the constraints for a larger range of inner core radii than interior models with a hot temperature profile. As a consequence of global mass conservation and due to the fact that the solid inner core is denser than the liquid outer core, the radius of the core decreases with increasing inner core radius. The hot models represent planets in which there is almost no sulfur in the core and in which the core is therefore denser.

Model name	CMB temper. (K)	ρ_m (kg/m³) min	max	r_{icb} (km) min	max	r_{cmb} (km) min	max
FC	1850	3336	3395	1	1810	1820	1976
	2000	3343	3355	1	1830	1837	1876
MA	1850	3275	3298	1	1820	1838	1983
	2000	3281	3285	1	1840	1850	1883
TS	1850	3314	3344	1	1860	1830	1978
	2000	3309	3317	1	1830	1843	1880
MC	1850	3224	3245	1	1840	1847	1988
	2000	3230	3233	1	1840	1859	1880
EC	1850	3093	3115	1350	1850	1870	2002

Table 3: Summary of the 9 interior models classes. Crust thickness is 50km and crust density is 2900 kg/m^3 for all models. See Rivoldini et al. (2009) and Rivoldini and Van Hoolst (2013) for more details on these models.

The spherical interior model is then transformed to a bi-axial model with equatorial flattening. We assume that Mercury has a rigid bi-axial mantle and a core that is in hydrostatic equilibrium with respect to the mantle. We specify the geometrical flattening at the top and bottom of the mantle (β_m and β_{cmb}), and we compute the flattening as a function of radius in the core in response to the flattened mantle, following the method described in the study of Dumberry et al. (2013). Flattening versus depth in the core is calculated under the assumption of hydrostatic equilibrium. In the following sections, we consider that $\beta_{cmb} = \beta_m$, $\beta_{cmb} = \beta_m/2$ and $\beta_{cmb} = 2\beta_m$. Once the ratio between β_m and β_{cmb} is chosen, the flattening of the whole planet is adjusted to match the observational constraints on $C_{22} = (B - A)/(4\,MR^2)$ obtained from measurements by MESSENGER (Smith et al., 2012). We use the mean value of C_{22} without assuming an error for all calculations. From the resulting core flattening with depth, the coupling strength's K, K_m and K_{ic} can be computed (Dumberry et al., 2013). With increasing inner core radius, the parameters K_{ic} and K increase while K_m decreases. The difference between the parameter values for the 3 flattening assumptions is less than 2% for K_m, between 14% and 30% for K_{ic}, and up to more than 50% for K.

2. Results

2.1. Periods of the eigenmodes and resonance

The first free mode T_1 (from Eq. (11)) represents the free libration of the combined mantle and inner core. Its period increases with inner core size (Fig. 1). Without an inner core, this mode reduces to the mantle free libration period $2\pi/\omega_m$ (Eq. (10)) and its period is between 11.4 and 13.4y. For $\beta_{cmb} = \beta_m$, the period T_1 is between 11.4 and 17.7y, approaching the value of about 18y for an almost fully solid Mercury. It stays very close to $2\pi/\omega_m$ for small inner cores but significantly differs from the mantle libration period for inner cores larger than about 1000 km. The effect of the flattening assumption on the first free period is very small: for $\beta_{cmb} = \beta_m/2$, T_1 varies between 11.4 and
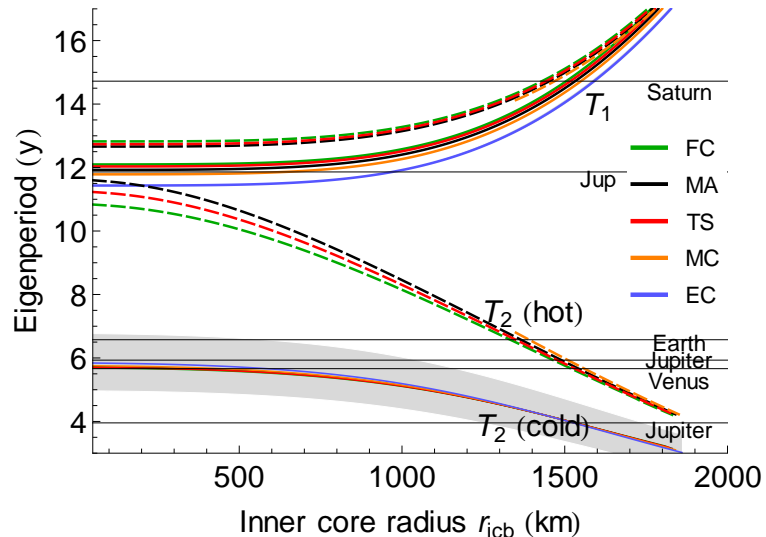

Figure 1: Periods of the two eigenmodes (T_1, T_2) as a function of the inner core size. The different curves represent the 9 different interior models classes. The dashed curves represent the 4 models with the hot temperature profile. The light gray areas show the spread of the free libration periods resulting from the flattening assumption, for the TS class of interior model. In this gray area, the flattening assumptions varies from $\beta_{cmb} = 2\beta_m$ (lower limit) to $\beta_{cmb} = \beta_m/2$ (upper limit). The gray area is almost invisible around T_1. The horizontal black lines show the 6 main periods of the planetary perturbations. The orange dashed curve does not extend below 1350km because for this particular mantle mineralogy (MC) and the hot temperature profile, it is not possible to find interior models with a small inner core that fulfill the mass and radius constraints.

18y and between 11.4 and 17.6y for $\beta_{cmb} = 2\beta_m$. We plot in Fig. 1 a gray area covered by the different assumptions for the flattening, but this area is almost invisible.

The period of the second free mode T_2 (mantle-inner core gravitational mode) covers a very large range, depending on the mantle mineralogy, the temperature profile and the flattening assumption. Without mantle-inner core coupling, this mode does not exist. For $\beta_{cmb} = \beta_m$, T_2 is between 3 and 5.8y for interior models with a cold temperature profile and between about 4.1 and 11.6y for interior models with a hot temperature profile. In contrast to T_1, T_2 is significantly affected by the flattening assumption. The free period T_2 varies between 3.6 and 12.8y for $\beta_{cmb} = \beta_m/2$ and between 2.5 and 9.4y for $\beta_{cmb} = 2\beta_m$. Hence, T_2 increases with decreasing CMB flattening. In Fig. 1, the light gray area shows the large spread in the free libration periods resulting from the different flattening assumptions, for one class of interior models.

The period T_2 decreases with inner core size. This is because T_2 depends mainly on the strength of the mantle-inner core gravitational coupling (constant K), which depends primarily on the density contrast between the fluid and solid core at the ICB. In order to satisfy the constraints on Mercury's mass, models with large (pure Fe) inner core must have a larger weight fraction of sulfur in the fluid core and thus a larger density contrast at the ICB: the larger K then leads to a shorter T_2 period. As it can

be seen on Fig. 1, different interior density models result in vastly different T_2 periods. There is a clear separation between the hot and cold mantle models; for a given inner core size, hot models have a much lower sulfur fraction in the fluid core, and thus have a smaller K and a longer T_2 period.

The hot and cold temperature are plausible temperature profiles for the mantle of Mercury; any intermediary temperature profile would produce a T_2 curve that lies in between that of the hot and cold models of Fig. 1. However, as other temperature profiles are possible, the range of variation of T_2 can be appreciably larger. Lastly, we note that the determination of T_2 crucially depends on the radial variations in density in the core (Dumberry et al., 2013). Taking instead the density of the fluid and solid cores to be uniform and equal to their mean values, the range of T_2 values on Fig. 1 would be much narrower, from 2.8y to 5.2y.

When a planetary period is near one of the free periods, the libration amplitude at that frequency is resonantly amplified. Whether a large amplification by resonance occurs (i.e. intersection of T_1 or T_2 with a planetary orbit period, see the horizontal lines in Fig. 1) depends on the interior structure of Mercury, and the equatorial flattening with depth. For an inner core radius smaller than about 1000km, the period T_1 is very close to the orbital perturbation by Jupiter at 11.86y. A large inner core moves the free libration period T_1 further away from the 11.86y perturbation period, and would result in a smaller long-period forced libration amplitude. However, the free period T_1 could be very close to the orbital perturbation by Saturn (14.7y) if the inner core radius were approximately $1500-1600$ km. The free mode period T_2 may be resonant with the 3.95y, 5.66y, 5.9y and the 6.57y orbital perturbations. For hot interior models, the free period T_2 may be close to the 11.86y perturbation period for small inner cores.

2.2. Amplitude of the long-period forced librations

Since the forcing frequencies are known from the orbital theory (Table 1), we can compute the librations of the mantle and of the inner core for each of these frequencies. The amplitudes computed in this section included viscous coupling at both the CMB and the ICB ($k_m = k_{ic} = 10^{-5}$/y), no electromagnetic coupling and assumed a rigid inner core ($\tau \to \infty$). The level of amplification for each of the long-period forced librations differs for different interior models of Mercury. This is because each of these models have different coupling parameters K, K_m and K_{ic}, which affects the frequencies $\omega_{1,2,m,g,ic}$ on which the amplitude depends (see equation 18). Fig. 2 shows the absolute value of the 6 largest amplitudes of the long-period forced librations of the mantle ψ_m as a function of the inner core size for the case $\beta_m = \beta_{cmb}$. A large amplification by resonance occurs when, for a specific inner core radius, the period of one of the free modes is close to the period of an orbital perturbation. The main long-period
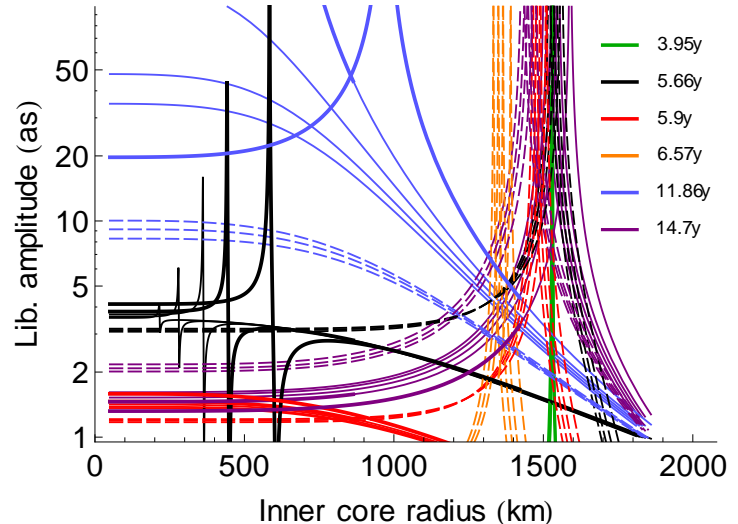

Figure 2: Absolute value of the amplitudes of the long-period forced variations of the rotation angle ψ_m as a function of the inner core size for 9 different classes of interior models, using damping parameters of $k_m = k_{ic} = 10^{-5}$/y and no viscous inner core deformation ($\tau \to \infty$). The different colors show the 6 main perturbing frequencies. We use dashed lines for the 4 classes of hot interior models. The outer core flattening is $\beta_{cmb} = \beta_m$. The thicker parts of the curves show the interior models for which the amplitude of the 88d libration falls within the 1-sigma interval of Margot et al. (2012). The amplitude of the 88d libration is about 38.5 as.

forced libration is the one due to Jupiter's perturbation on Mercury's orbit at 11.86y period (blue curves in Fig. 2). As in the case without inner core mantle coupling (see figure 5 of Yseboodt et al. 2010), a large amplification of this libration occurs for inner cores that are not too large. For an inner core radius smaller than 1200 km, the effect of the inner core on the eigenperiod T_1 is weak (Fig. 1), and the amplitude of the 11.86y libration depends mainly on the ratio $(B - A)/C_m$ which determines the free mantle libration period (see Eq. (10)). For hot interior models with small inner cores, the second free period T_2 can also be close to the 11.86y period. However because the resonance factor associated with T_2 ($\omega_m^2 - N$ coefficient in Eq. (19)) is typically about 10 times smaller than the resonance factor associated with T_1, the amplification in that case is much smaller.

Long-period forced librations at five other frequencies may also have an amplitude larger than a few arcsec: at 3.95y, 5.66y, 5.9y, 6.57y and 14.7y periods. If Mercury does not have an inner core, the amplitude of these librations are not amplified and always remain below 5 as. Since the difference between the free periods and these forcing periods changes faster with changing inner core radius than for the 11.86y libration (see Fig. 1) and since the amplitude of the planetary perturbation λ_i is small, these resonances occur over a narrower range of inner core radii.

As the inner core radius increases from 50 to 600 km, for the cold interior models, the 5.66y libration amplitude (black curves) varies from minus a few arcsec to $-\infty$ at

the point when T_2 is precisely equal to 5.66y. Once T_2 crosses 5.66y, the resonance factor changes sign (because of $\omega_2^2 - \omega_i^2$ in Eq. (19)) and the mantle libration amplitude jumps to $+\infty$. A further increase in inner core radius takes T_2 further away from the resonance and the mantle libration decreases back to minus a few arcsec. The quantity plotted in Fig 2 is the absolute value of this amplitude, so it is remains positive. However, note that the mantle libration amplitude passes through zero for a specific inner core radius. This marks the location where the planetary forcing on the mantle is equal and opposite to the gravitational torque by the inner core. This does not occur precisely at $T_2 = 5.66y$, but when T_2 is slightly offset (and smaller). This effect is more visible for the 5.66y period than for other orbital periods because it has the largest orbital perturbation (see Table 1). For other orbital frequencies, since the orbital perturbations λ_i are much smaller, the amplitudes far from the resonant frequencies are very small (close to zero) and the change of sign happens for libration amplitude smaller than 1 as, outside the graph limits.

In order to get the flattening of the mantle, we use the mean value of C_{22} from Smith et al. (2012) without assuming an error. A different choice of C_{22} within its 3σ error bound largely affects the amplitude and location of the resonance because C_{22} determines the amplitude of the planetary flattening, and therefore it affects the values for K, K_m, and K_{ic}. Because the free period T_2 is very sensitive to the flattening assumption, a small change in the core equatorial flattening induces a change in the position of the resonance and the level of amplification. The choice of the β_{cmb}/β_m ratio has the strongest effect on the resonance of the 3.95y, 5.9y and 6.57y periods. For the other orbital periods, the choice of the interior model is more important. As Fig. 2 illustrates, the amplitudes of the long-period forced librations cannot be predicted with any reasonable precision because of their strong dependence on interior parameters of Mercury for which we do not have good constraints. Nevertheless, some general observations can be made. For inner cores smaller than about 1200 km, the 11.86y libration is expected to have a forced libration amplitude of at least about 10 as. Its amplitude decreases to about 1 as for interior models with very large inner cores. Detection of this forced libration might thus be used to distinguish between very large inner core or not. If a large amplitude of the 14.7y libration is detected with a precision of a few arcseconds, then it means that the inner core is large (radius between 1300 and 1600 km). The amplitude of the 3.95y libration might be large only if the inner core is very large. However, this is a very narrow resonance. Finally, a very narrow resonant amplification of the 3 other planetary frequencies is possible for large or small inner core radius depending on whether the temperature of the mantle is hot, mild or cold.

The interior models in Fig. 2 cover a large range of $(B-A)/C_m$ values, and therefore a large range of 88d libration amplitudes. However a recent fit of the 88d libration amplitude to the rotation data (Margot et al., 2012) gives a 1-sigma interval for this amplitude of $[36.9 - 40.1]$ as. Models that agree with the 1 sigma interval of the 88d libration are represented by thick lines in the figure 2. If we extend the uncertainty interval to a 3-sigma interval, then the number of allowed interior models is much larger: almost all the models in the figure are allowed.

Figure 3 shows the amplitudes of the angular rotation velocity variations $\dot{\psi}_m$ (Eq. 18) for the same 6 orbital perturbation frequencies and for the different interior models. Resonant amplifications are present at the same frequen-
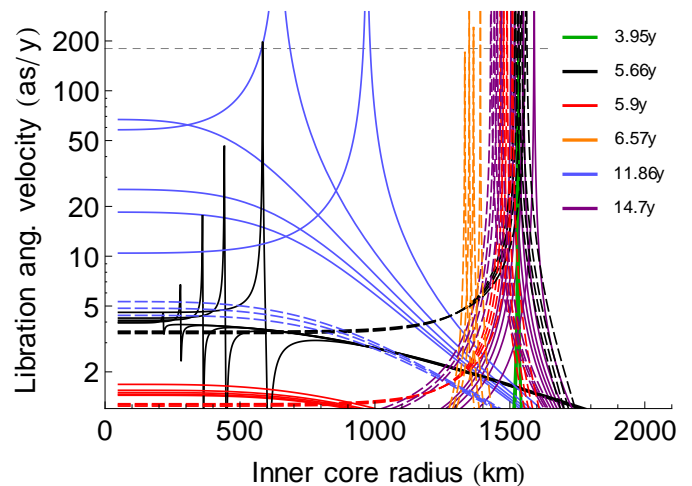

Figure 3: Absolute value of the amplitudes of Mercury's long-period librational angular velocity $\dot{\psi}_m$ for 9 different classes of interior models and for the 6 main orbital frequencies. The configuration is the same as for Fig. 2. The amplitude of the 88d angular velocity is of the order of 1000 as/y (out of the boundaries of the figure). The horizontal dashed line shows the current uncertainty on the radar observations.

cies as the libration angle for specific interior models (see Fig. 2). Their amplitude is usually smaller than 80 as/y, except for a very small range of interior models.

2.3. Effect of the dissipation

Calculations for different choices of k_m and k_{ic} than the nominal values $k_m = k_{ic} = 10^{-5}$/y show that, provided k_m and k_{ic} are not larger than approximately 10^{-3}/y, the only difference with the results presented in the previous section is a reduction of the peak amplitude of libration at the resonance periods. As discussed in section 1.5, the addition of EM coupling at the CMB should not alter the amplitude of k_m significantly, whereas EM coupling at the ICB could lead to an amplitude of k_{ic} of the order of 10^{-3}/y for reasonable assumptions about the magnetic field strength. Therefore, except at the precise location of resonances, the results for the nominal case presented above are not largely affected by the nature and amplitude of coupling at the CMB and ICB. The maximal amplitude of the peak may be approximated by Eq. (34). The damping parameter k_m has a larger effect than the damping parameter k_{ic} on the libration amplitude of the mantle and of the

10

inner core. This effect is also observed in the maximal amplitude for ψ_m. This can be understood from the expression (Eq. (34)) of the maximal amplitude for ψ_m: in the denominator, the coefficient in front of the damping parameter k_m is much smaller than the one in front of k_{ic}. Dissipation can significantly change the phase of the libration but since the electromagnetic and viscous couplings are usually smaller than the gravitational coupling, this only happens if a planetary perturbation frequency is very close to the free mode frequency. If the differences between the frequencies $\omega_1 - \omega_i$ and $\omega_2 - \omega_i$ are larger than about 0.002 rad/y, the phase angle ϕ_{ψ_i} (Eq. (33)) reduces to ϕ_{λ_i} or to $\phi_{\lambda_i} + 180°$ (the value depends on the sign of the frequency differences) with an error of less than $0.2°$ for the nominal value of the dissipation parameters. The widths of the resonance peaks depend mostly on the amplitude of the planetary perturbations λ_i and only very slightly on the damping parameters.

Calculations with different choices of the inner core viscous relaxation time τ show that, provided τ is larger than about 25 years, the main difference in the results is a reduction of the peak amplitude of librations at the resonance. Thus, except for inner core radii where the free period T_1 or T_2 almost matches a planetary forcing period, our results in the previous section are barely sensitive to the precise value of τ. However, if τ is of the order of about 25y or less, then the amplitude of the long-period librations are reduced for a much broader range of inner core radii. If τ is less than a few years, then the amplitudes of the long-period librations are almost reduced to the original orbital perturbation λ_i. The phases of the long-period librations are also largely changed.

2.4. Link with the observations

The amplitude of the 88d forced libration (38.5 as, Margot et al. 2012) has approximately the same order of magnitude as the long-period forced librations (see Fig. 2). This is not the case for the amplitudes of the angular rotation velocity variations $\dot{\psi}_m$ (see Fig. 3): the 88d amplitude is about 1000 as/y, about 10 to 100 times larger than the long-period amplitudes. This is due to the temporal derivative that leads to more prominent short-period effects in the rotation rate than in the libration angle. The long-period librations will be more difficult to detect in spin radar data than in orientation data.

These amplitudes may also be compared to the present uncertainty on the observations of the rotation state of Mercury. The average precision on the rotation rates obtained with Earth-based radar data (Margot et al., 2012) is of the order of 180 as/y. Fig. 3 shows that a velocity amplitude larger than 180 as/y only occurs under a very specific range of inner core radii (except in the case of the 11.86y libration period for which the signature may be detectable over a larger range of inner core radii). Given the current observational precision, it follows from the calculated libration velocities, that a large difference between

models with and without inner core coupling can only be seen if Mercury happens to be close to a resonance.

The libration angle can also be measured directly. A measurement of the libration amplitude was recently provided by Stark et al. (2012) using MESSENGER data with an uncertainty on the 88d libration amplitude of about 5 as. The expected precision on the libration angle with the BepiColombo spacecraft is about 1 arcsecond (Pfyffer et al., 2011). Fig. 2 shows that libration signatures for a large fraction of interior models would exceed a few arcseconds and would therefore be detectable. Therefore, the influence of the inner core in the long-period forced librations has a better chance to be detected on the basis of future observations of the libration angle rather than the rotation rate.

In order to gain pertinent inferences about the interior structure of Mercury, one would need arcsecond precision observations of the libration angle over a time interval long enough to identify the planetary periods, i.e., 5-15y. Clearly, predictions of the long-period forced librations from our model depend on many parameters that are not well known such as the inner core size, the interior density structure, etc. Different combination of these parameters can generate long-period librations of equivalent amplitudes. Nevertheless, despite the non-uniqueness, the constraint of matching predicted with observed long-period librations would reduce the possible parameter space and thus provide valuable information on Mercury's interior.

The 88d libration amplitude of the inner core γ_{ic} is much smaller than the 88d libration amplitude of the mantle (Van Hoolst et al., 2012). The amplitude of the 88d libration is between 0.5 and 2.2 as, depending on the interior model and the flattening assumption. At semi-annual period, the inner core libration is below 0.2 as (Van Hoolst et al., 2012). However, the long-period librations of the inner core may also be largely amplified, for the same frequencies as the mantle libration since the denominators in the equations for the libration amplitude are the same for the inner core and for the mantle (Eqs. (16) and (17)). Although inner core librations could in principle be detected through their effect on the degree-two, order-two gravitational coefficient C_{22}, the signal is probably too weak to be observed in the near future by either MESSENGER or BepiColombo.

3. Fit of the radar data

In this section, we investigate whether including the coupling between the mantle and inner core can improve the fit to the radar data of Margot et al. (2012) and determine whether it is possible to constrain the size of the inner core from the measurements of the rotation rate.

Earth-based radar measurements of the instantaneous spin state of Mercury have been made at 35 different epochs between 2002 and 2012 (Margot et al., 2012). From the correlation of the radar echo signals at two Earth stations, Margot et al. (2012) obtained 35 instantaneous spin rate

values. Currently, the averaged uncertainty on these rotation rates is about 180 as/y. Since two polarizations have been recorded, two data points and the associated uncertainties are available at each epoch.

We fit the observed rotation rates with a rotation model for Mercury that includes the short-period forced librations (annual, semi-annual, etc., see section 1.6) and the long-period forced librations. The model also includes dissipation at the CMB and ICB (damping parameters $k_m = k_{ic} = 10^{-5}$/y). We assume that the two free librations have not been excited recently (e.g. by an internal forcing, Koning and Dumberry 2013) and have attenuated to a negligible amplitude. Adding a free libration would also complicate the analysis by introducing additional parameters to estimate and by a possible overlap with the 11.86y libration. In order to compare the solution without an inner core with a situation with an inner core, we use as an estimator of the goodness of the fit the reduced χ^2 (sum of the squares of the differences between the model and the data expressed in units of the uncertainty, divided by the number of degrees of freedom). We seek a global minimum of the reduced χ^2 for all the interior models.
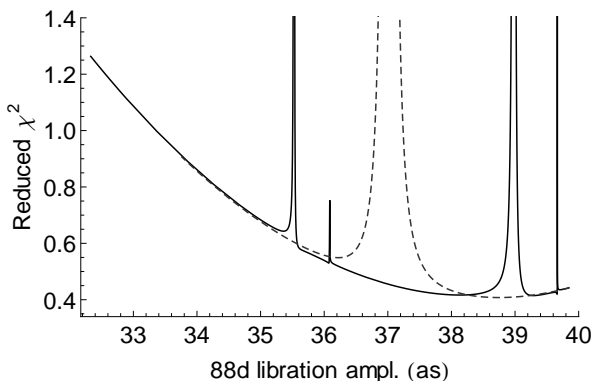

Figure 4: Reduced χ^2 as a function of the annual libration amplitude for the EC interior model class with a cold temperature profile. The inner core radius increases from right to the left. The assumption for the flattening is $\beta_{cmb} = \beta_m$. The black (dashed) line shows the reduced χ^2 using a rotation model with (without) inner core coupling.

Fig. 4 shows that the main effect on the reduced χ^2 is the 88d libration amplitude. The reduced χ^2 has a strong dependence on the 88d libration amplitude, both for interior models that take into account the mantle-inner core coupling and for those that do not. Additionally we see that the long-period forced librations increases the reduced χ^2 for very specific interior models. To match the constraints on Mercury's mass, models with large inner core have smaller outer core radius; this leads to an increase in C_m and thus a decrease in $(B - A)/C_m$ and in the 88d amplitude. Therefore the interior models with small inner cores have 88d libration amplitude larger than 39 as in Fig. 4 while models with large inner cores have a 88d libration amplitude smaller then 35 as.

In general, the inclusion of mantle-inner core coupling

in the rotation model does not improve the best fit (Fig. 4). The global minimal reduced χ^2 is about 0.4, which is about the same as for the situation without mantle-inner core coupling. The effects of a small inner core (radius smaller than about 500km) on the rotation model are usually so small that the rotation models with and without mantle-inner core coupling produce almost the same χ^2. However if a resonance between one of the free modes and one of the planetary perturbation periods occurs for some particular interior model, the amplitude of the long-period libration becomes very large and the fit is usually degraded. Thus, based on the reduced χ^2 analysis, we conclude that the radar observations suggest that Mercury's librations do not contain large, resonantly amplified, long-period forced librations. Other flattening assumptions change the position of the resonances, but do not globally decrease the reduced χ^2.
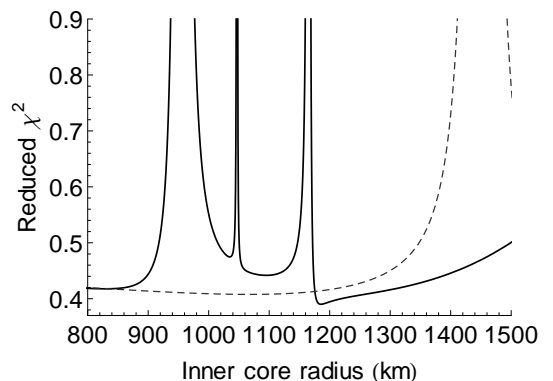

Figure 5: Reduced χ^2 as a function of the inner core radius for the EC interior model and a cold temperature profile (see Rivoldini et al. 2009 for details). The assumption for the flattening is $\beta_{cmb} = \beta_m/2$ and $C_{22} = 8.088 \times 10^{-6}$. The black (dashed) line shows the reduced χ^2 using a rotation model with (without) mantle-inner core coupling. We see that a global minimum for the reduced χ^2 is when the inner core radius is 1186km, indicating the best fit model.

Some interior models have been found that have a reduced χ^2 smaller than 0.4 when inner core coupling is included. For example, the reduced χ^2 is 0.39 (see Fig. 5) if $\beta_{cmb} = \beta_m/2$, $r_{icb} = 1186$ km and using a cold mantle with a low density (EC model of Rivoldini et al. 2009). This is due to a resonance between the 5.66y perturbation and the free period T_2. For some specific inner core radii close to 1186km, an amplitude of 23 as for the 5.66y libration allows for a better fit to the observations. However, the improvement in the fit is extremely sensitive to the precise amplification of the 5.66y libration: a small increase in the amplification leads to a large reduced χ^2 and degrades the fit dramatically.

If we explore the confidence interval for C_{22} and the other parameters of our model, it is also possible to find very sharp resonances that can, for very specific interior model and inner core radius, slightly decrease the reduced χ^2.

The effect of the inner core can therefore provide a

slightly better fit to the data for specific interior structure models. However, the improvement is only marginal and it cannot be reasonably argued that they provide a better match to the libration observations. The uncertainty on the available data is presently too large to be sensitive to the effect of mantle-inner core coupling and by extension, to the size of the inner core. Additionally, the time period covered by the available data is too short to separate the different libration amplitudes. Since a dramatic worsening of the fit may occur at resonances, we can only conclude that a very large amplification is most likely not present in Mercury's librations. Based on this, combinations of interior parameters that would yield a free mode period very close to one of the main long-period librations must be rejected.

4. Conclusion

We presented a theory to compute the amplitude and phase of the long-period forced librations of Mercury. These long-period librations are caused by the planetary perturbations on the orbit of Mercury. Our model takes into account the internal coupling that occurs between the solid inner core, fluid outer core and mantle. This includes gravitational and pressure torques between these layers, as well as viscous and electromagnetic couplings at the CMB and ICB. Our model also includes viscous deformation of the inner core.

Previous studies that have investigated the long-period forced librations of Mercury did not take into account the coupling dynamics of the inner core with the rest of the planet. The inclusion of the inner core leads to two eigen modes that have a large range of possible periods. Their precise periods depend on the interior structure, including the size of the inner core. Large amplification of a long-period forced libration occurs if its period is close to one of the free mode periods. Our results show that for a large set of models, long-period forced librations may have an amplitude well above 5 arcsec. For a small inner core radius, the first free period T_1 is close to the Jupiter perturbation period at 11.86y while for a large inner core, it can be closer to Saturn orbital perturbation at 14.7y. The second free period may be resonant with several orbital perturbations: 3.95y, 5.66y, 5.9y, 6.57y and even the 11.86y perturbation. Except very close to resonance periods, the long-period forced librations are not sensitive to the strength and nature of the coupling at the CMB and ICB if the damping parameters k_m and k_{ic} are smaller than 10^{-3}/y. Our results are also insensitive to viscous deformation within the inner core, except for the maximal amplitude of the resonances peaks, provided they occur on a characteristic timescale longer than 25y.

We also tested whether the inclusion of an inner core can provide a better fit to the Earth based radar observations of Mercury's rotation rate. Because the long-period forced librations have amplitudes that are below the current uncertainty on these observations and because the time interval they cover is short compared to the main planetary forcing periods, the data are not very sensitive to these long-period forced librations. Therefore, it is not possible to detect the dynamical influence of the inner core on Mercury's forced librations on the basis of the currently available observations, other than the fact that very large forced libration amplitude at planetary periods are not suggested by observations.

The amplitude of the long-period forced librations predicted by our model are sufficiently large to be measurable by spacecraft observations of the libration angle of Mercury. This is provided the libration angle is observed for a sufficiently long time window and with a precision of a few arcseconds. Depending on their precision, future measurements of long-period forced librations might then allow us to place useful constraints on the interior structure of Mercury. As we have shown in our study, the combination of parameters (inner core size, interior profiles of flattening and density, etc) that can generate a given libration is non-unique. Nevertheless, matching predicted and observed long-period forced librations would reduce the possible parameter space and thus provide valuable information on Mercury's interior.

References

Anderson, B. J., Johnson, C. L., Korth, H., Purucker, M. E., Winslow, R. M., Slavin, J. A., Solomon, S. C., McNutt, R. L., Raines, J. M., Zurbuchen, T. H., 2011. The Global Magnetic Field of Mercury from MESSENGER Orbital Observations. Science 333, 1859–1862.

Buffett, B. A., 1992. Constraints on magnetic energy and mantle conductivity from the forced nutations of the earth. J. Geophys. Res. 97, 19581–19597.

Buffett, B. A., 1998. Free oscillations in the length of day: inferences on physical properties near the core-mantle boundary. In: Gurnis, M., Wysession, M. E., Knittle, E., Buffett, B. A. (Eds.), The core-mantle boundary region. Vol. 28 of Geodynamics series. AGU Geophysical Monograph, Washington, DC, pp. 153–165.

Constable, S., 2007. Geomagnetism. In: Schubert, G., Kono, M. (Eds.), Treatise on geophysics. Vol. 5. Elsevier, Amsterdam, Ch. 7, pp. 237–276.

de Wijs, G. A., Kresse, G., Vočadlo, L., Dobson, D., Alfè, D., Gillan, M. J., Price, G. D., 1998. The viscosity of liquid iron at the physical conditions of the Earth's core. Nature 392, 805–807.

Deng, L., Seagle, C., Fei, Y., Shahar, A., 2013. High pressure and temperature electrical resistivity of iron and implications for planetary cores. Geophys. Res. Lett. 40, 33–37.

Dufey, J., Lemaître, A., Rambaux, N., 2008. Planetary perturbations on Mercury's libration in longitude. Celestial Mechanics and Dynamical Astronomy 101, 141–157.

Dumberry, M., 2011. The free librations of Mercury and the size of its inner core. Geophys. Res. Lett. 38, L16202–.

Dumberry, M., Rivoldini, A., Van Hoolst, T., Yseboodt, M., 2013. The role of Mercury's core density structure on its longitudinal librations. Icarus 225 (1), 62 – 74.

Grott, M., Breuer, D., Laneuville, M., 2011. Thermo-chemical evolution and global contraction of mercury. Earth and Planetary Science Letters 307, 135–146.

Kaula, W. M., 1966. Theory of satellite geodesy. Applications of satellites to geodesy. Waltham, Mass.: Blaisdell.

Koning, A., Dumberry, M., 2013. Internal forcing of Mercury's long period free librations. Icarus 223, 40–47.

Margot, J. L., Peale, S. J., Jurgens, R. F., Slade, M. A., Holin, I. V., 2007. Large longitude libration of mercury reveals a molten core. Science 316 (5825), 710–714.

Margot, J.-L., Peale, S. J., Solomon, S. C., Hauck, II, S. A., Ghigo, F. D., Jurgens, R. F., Yseboodt, M., Giorgini, J. D., Padovan, S., Campbell, D. B., 2012. Mercury's moment of inertia from spin and gravity data. Journal of Geophysical Research (Planets) 117, E00L09–.

Ness, N. F., Behannon, K. W., Lepping, R. P., Whang, Y. C., 1975. The magnetic field of Mercury. I. J. Geophys. Res. 80, 2708–2716.

Peale, S. J., 2005. The free precession and libration of Mercury. Icarus 178, 4–18.

Peale, S. J., Margot, J. L., Yseboodt, M., 2009. Resonant forcing of Mercury's libration in longitude. Icarus 199, 1–8.

Peale, S. J., Phillips, R. J., Solomon, S. C., Smith, D. E., Zuber, M. T., 2002. A procedure for determining the nature of Mercury's core. Meteoritics and Planetary Science 37, 1269–1283.

Pfyffer, G., Van Hoolst, T., Dehant, V., 2011. Librations and obliquity of Mercury from the BepiColombo radio-science and camera experiments. Planetary and Space Science 59, 848–861.

Rivoldini, A., Van Hoolst, T., 2013. The interior structure of Mercury constrained by the low-degree gravity field and the rotation of Mercury. Earth and Planetary Science Letters, submitted.

Rivoldini, A., Van Hoolst, T., Verhoeven, O., 2009. The interior structure of Mercury and its core sulfur content. Icarus 201, 12–30.

Rivoldini, A., Van Hoolst, T., Verhoeven, O., Mocquet, A., Dehant, V., 2011. Geodesy constraints on the interior structure and composition of Mars. Icarus 213, 451–472.

Smith, D. E., Zuber, M. T., Phillips, R. J., Solomon, S. C., Hauck, S. A., Lemoine, F. G., Mazarico, E., Neumann, G. A., Peale, S. J., Margot, J.-L., Johnson, C. L., Torrence, M. H., Perry, M. E., Rowlands, D. D., Goossens, S., Head, J. W., Taylor, A. H., 2012. Gravity Field and Internal Structure of Mercury from MESSENGER. Science 336, 214–217.

Standish, E. M., 1998. JPL planetary and lunar ephemerides, de405/le405. Iom (IOM 312.F-98-048).

Stark, A., Oberst, J., Preusker, F., Gwinner, K., Peale, S. J., Margot, J. L., Zuber, M. T., Solomon, S. C., 2012. A Technique for Measurements of Physical Librations from Orbiting Spacecraft: Application to Mercury. In: European Planetary Science Congress 2012, held 23-28 September, 2012 in Madrid, Spain. pp. EPSC2012-254.

Van Hoolst, T., Rambaux, N., Karatekin, Ö., Dehant, V., Rivoldini, A., 2008. The librations, shape, and icy shell of Europa. Icarus 195, 386–399.

Van Hoolst, T., Rivoldini, A., Baland, R.-M., Yseboodt, M., 2012. The effect of tides and an inner core on the forced longitudinal libration of Mercury. Earth Planet. Sci. Lett. 333, 83–90.

Veasey, M., Dumberry, M., 2011. The influence of Mercury's inner core on its physical libration. Icarus 214, 265–274.

Verhoeven, O., Tarits, P., Vacher, P., Rivoldini, A., Van Hoolst, T., 2009. Composition and formation of Mercury: Constraints from future electrical conductivity measurements. Planetary and Space Science 57, 296–305.

Yseboodt, M., Margot, J.-L., Peale, S. J., 2010. Analytical model of the long-period forced longitude librations of Mercury. Icarus 207, 536–544.